Magnetotransport in single-crystal half-Heusler compounds

K. Ahilan,[1] M. C. Bennett,[1] M. C. Aronson,[1] N. E. Anderson,[2] P. C. Canfield,[2] E. Munoz-Sandoval,[3,4] T. Gortenmulder,[3] R. Hendrikx,[3] and J. A. Mydosh[3,5]

[1]*University of Michigan, Ann Arbor, Michigan 48109, USA*

[2]*Ames Laboratory, Iowa State University, Ames, Iowa 50011, USA*

[3]*Kamerlingh Onnes Laboratory, Leiden University, Leiden, The Netherlands*

[4]*Advanced Materials Department, IPICyT, Apartado Postal 3-74, 78231 San Luis Potosi, San Luis Potosi, Mexico*

[5]*Max Planck Institute for Chemical Physics of Solids, Dresden, Germany*

(Received 5 October 2003; revised manuscript received 12 December 2003; published 28 June 2004)

We present the results of electrical resistivity and Hall effect measurements on single crystals of HfNiSn, TiPtSn, and TiNiSn. Semiconducting behavior is observed in each case, involving the transport of a small number of highly compensated carriers. Magnetization measurements suggest that impurities and site disorder create both localized magnetic moments and extended paramagnetic states, with the susceptibility of the latter increasing strongly with reduced temperature. The magnetoresistance is sublinear or linear in fields ranging from 0.01–9 T at the lowest temperatures. As the temperature increases, the normal quadratic magnetoresistance is regained, initially at low fields, and at the highest temperatures extending over the complete range of fields. The origin of the vanishingly small field scale implied by these measurements remains unknown, presenting a challenge to existing classical and quantum mechanical theories of magnetoresistance.

DOI: 10.1103/PhysRevB.69.245116 PACS number(s): 71.20.Lp, 71.20.Nr

One of the most exotic settings for small gap insulators is among materials made entirely of metals, i.e., intermetallic compounds. Nonetheless, it was demonstrated in the early 1990's that a subset of the half-Heusler compounds, with the generic formula RNX (R,N are transition metal elements and X is a main group element), display semiconducting transport while infrared absorption experiments found semiconducting gaps with magnitudes of $\sim$100 meV or less.[1,2] In subsequent years, these materials were found to have a substantial thermopower[2,3] and a number of different compositions were explored[4–8] in the hopes of optimizing these characteristics. Virtually all of these experiments were carried out on polycrystalline samples, and since annealing dramatically affected their transport properties,[2,4] it was clear that the samples were unlikely to be either stoichiometric, or single phase. Understanding the fundamental properties of these unusual materials, and in particular how they are affected by defects and impurities, is clarified by the study of single crystal samples, which we report in detail here.

Many intermetallic compounds form in the Heusler structure RN_2X, with four interpenetrating face centered cubic lattices, where the N elements lie at the center of the rock-salt cube formed by the R and X elements. The half-Heuslers are a variant on this structure, where one of the sublattices is entirely vacant, implying that now the N atoms ideally occupy every other rock-salt cube. This MgAgAs structure is found in intermetallic compounds with 16–20 electrons per formula unit z, but most often when $z=18$ as in the RNiSn (R=Ti, Zr, and Hf).[9] Of the known half-Heusler compounds,[10] only a few are thought to be insulating in the absence of disorder: RNiSn (R=Ti, Zr, and Hf) and RNSn (R=Zr and Hf, N=Pd and Pt),[1] LnPdSb (Ln=Ho, Er, Dy),[6] LnPtSb (Ln=trivalent rare earth),[8] CoTiSb and CoNbSn,[7] and NbIrSn.[5] Studies of half-Heusler systems in which the electron count is changed systematically[7,11,12] reveal that insulating behavior is generally observed near $z=18$, while metallic and sometimes magnetically ordered systems are found at both higher and lower electron counts. We note that this phenomenological result is based largely on resistance measurements carried out on polycrystalline samples, although a report on a single crystal of TiNiSn has been made.[1] Disorder, particularly involving site interchange, is likely to be a complicating and inherent feature of the half-Heusler family,[1,4] suggesting that measurements on single crystals may simplify the interpretation of experimental results. However, electronic structure calculations[13] support the view that the semiconducting behavior found in the RNiSn (R=Ti, Zr, Hf) is an intrinsic feature, finding indirect gaps between the Γ and X points in each compound. The gap is determined by the strength of the R-Sn pd hybridization, which leads to anticrossing of the extrema of the conduction and valence bands, which have primarily R d_{xy} character. The anticrossing is further amplified through an indirect interaction of the R states mediated by low lying Ni states. Nonetheless, the indirect gaps in TiNiSn, ZrNiSn, and HfNiSn are expected to be nearly identical, $\sim$0.5 eV.

The purposes of this paper are twofold. First, we report the results of transport and magnetization experiments on single crystals of TiNiSn, HfNiSn, and TiPtSn. For comparision, similar experiments were carried out on polycrystalline samples as well. These measurements show that the semiconducting behavior found in both polycrystalline and single crystal samples is intrinsic to HfNiSn, TiNiSn, and TiPtSn. Electron microscopy evidence is presented which reveals substantial metallurgical phase separation in all polycrystalline samples, removed by annealing. While the electrical resistivity of the single crystals is large and semiconducting, we find that impurities and defects play a pronounced role in the low-temperature properties of the single crystals. All of the samples, both single crystal and polycrystalline, are

weakly magnetic, due to the presence of both extended and localized moment bearing defect states. The Hall constant is unusually small, suggesting a near balance of electrons and holes. We find in addition that the magnetotransport is anomalous in this family of compounds. The second section of this paper is devoted to a description of the linear magnetoresistance found above a field scale which grows linearly with temperature, and which varies only moderately among our different samples.

Polycrystalline samples of HfNiSn were prepared by arc melting in a high purity Ar atmosphere, followed by high temperature vacuum annealing. An electron backscattering image of the as cast material is shown in Fig. 1(a), revealing that most of the sample is near-stoichiometric HfNiSn, but that there are additional phases at the boundaries of the grains. Microprobe measurements find that these phases are roughly equal quantities of Hf_5Sn_4 and the Heusler compound $HfNi_2Sn$, together making up about 4% of the total as cast sample volume. After annealing the as cast material in vacuum at 1000 °C for 720 h,[1] the grain boundary phases are much reduced in volume [Fig. 1(b)], and we presume that the composition of the grains approaches the stoichiometric level. Annealing had very similar effects on both TiNiSn and ZrNiSn polycrystals, which were found to undergo even more extensive phase separation. We also attempted to introduce B, Ta, Lu, Co, Mn, U, and Ce into HfNiSn and ZrNiSn as dopants. In every case, microprobe measurements showed that the dopants were segregated in the grain boundary phases, with no measurable solubility in the HfNiSn and ZrNiSn grains. We note that earlier efforts to dope the *R*NiSn also employed some of these elements,[4,10,14] and our results suggest that the primary effects of doping observed in these works likely result from modifications to the conducting properties of the grain boundary phases, and not from changes in the *R*NiSn matrix itself. We also experimented with shorter anneals at higher temperatures. Figure 1(c) shows that a 72 h anneal at 1300 °C significantly decreases the volume of grain boundary phases, which is now largely Hf_5Sn_4, although higher levels of $HfNi_2Sn$ and significant Sn loss from the matrix are observed near the surface of the polycrystalline sample. Due in part to these concerns about sample homogeneity, single crystals of HfNiSn were prepared at the University of Amsterdam/Leiden University ALMOS facility using the tri-arc assisted Czolchralski method, while single crystals of TiNiSn and TiPtSn were synthesized at Ames Laboratory from a Sn flux.[15] The crystal structures of all HfNiSn samples, both single crystal and polycrystal, were verified to be the MgAgAs type by powder x-ray diffraction. Backscattering images of the single crystals were completely featureless, finding no evidence for secondary phases.

We have studied these samples using both magnetization measurements, carried out using a Quantum Designs SQUID magnetometer, and electrical transport measurements, which employed both a Quantum Designs Physical Phenomena Measurement System and homebuilt helium cryostat systems. The resistivity and Hall effect measurements were performed at a frequency of 17 Hz, in the conventional four-probe and five probe configurations, respectively. Sweeps in positive and negative fields were combined to separate the mixed Hall signal and longitudinal magnetoresistance at each temperature. Special care was taken to avoid heating by the measuring current, especially at the lowest temperatures.

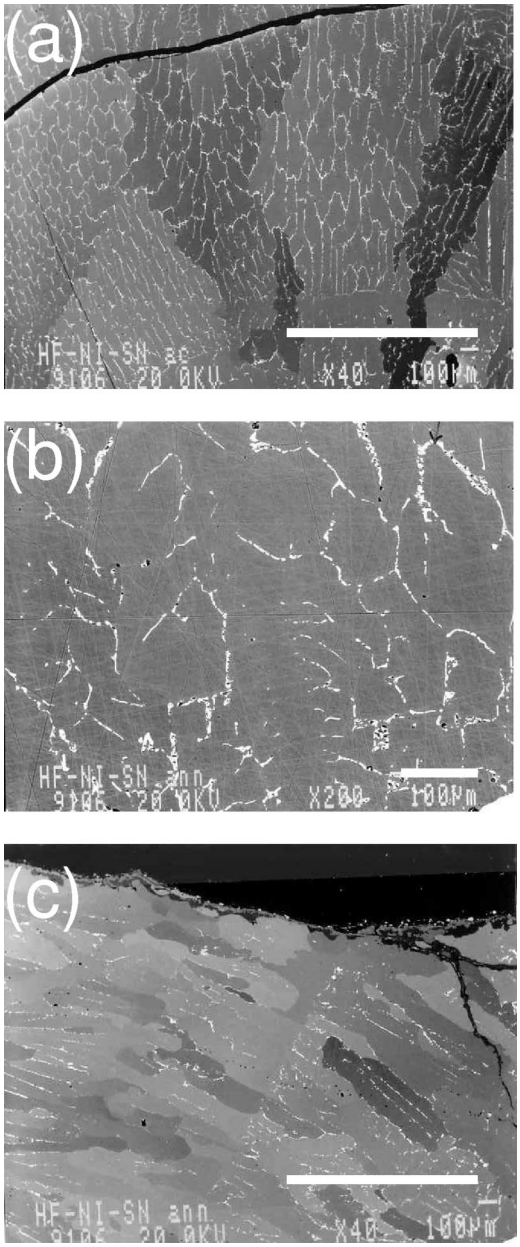

FIG. 1. Electron backscattering images of as cast polycrystalline HfNiSn (a), and after annealing for 720 h at 1000 °C (b), and for 72 h at 1300 °C (c). The white lines in each panel indicate a length of 100 microns.

Sample homogeneity has a profound effect on the transport observed in the half-Heuslers. Figure 2 depicts the temperature dependent resistivity for four different samples of HfNiSn: single crystal, as cast polycrystal, and polycrystal annealed for 720 h at 1000 °C (optimally annealed), and 72 h at 1300 °C. The resistivity increases slowly with decreasing temperature in the as cast material and reaches a broad maximum near 120 K, before decreasing and displaying a superconducting transition near 3.8 K. The superconductivity is easily suppressed with modest fields, and since it

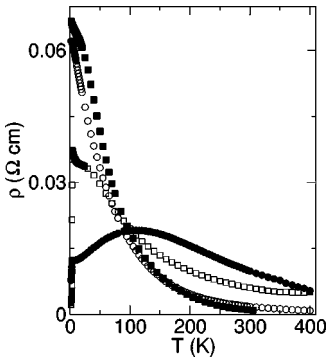

FIG. 2. The temperature dependent resistivity ρ for as cast polycrystalline HfNiSn (filled circles), annealed polycrystalline HfNiSn (open circles: 720 h at 1000 °C; open squares: 72 h at 1300 °C), and for a single crystal of HfNiSn (filled squares). Note that the resistivity of the HfNiSn single crystal has been divided by 25 for comparison to the polycrystalline samples.

is absent in the optimally annealed and single crystal samples we ascribe it to the grain boundary phases, or to trace amounts of elemental Sn. The resistivity of the optimally annealed polycrystalline sample reproduces the insulating behavior of the single crystal, although its resistivity is more than an order of magnitude smaller for the entire temperature range. The 72 h/1300 °C anneal has an intermediate effect, marginally increasing the measured resistivity over that of the as-cast sample, while rendering it insulating down to the superconducting transition. We conclude from the data in Fig. 2 that the grain boundary phases are highly conducting relative to the matrix, but that once they are removed by annealing HfNiSn is intrinsically a semiconductor, as previously claimed on the basis of experimental evidence gathered from the polycrystalline samples[1] and a single crystal of TiNiSn.[16]

Despite their intermetallic character, the single crystals of HfNiSn, TiNiSn, and TiPtSn all display semiconducting behavior, as predicted for filled *d*-band half-Heuslers.[13] Figure 3(a) shows the temperature dependences of the electrical resistivity of samples of all three materials, showing the behavior typical of *n*-type semiconductors. The activation plots of Fig. 3(b) are not linear over the entire range of temperatures investigated. In every case, the resistivity slowly approaches

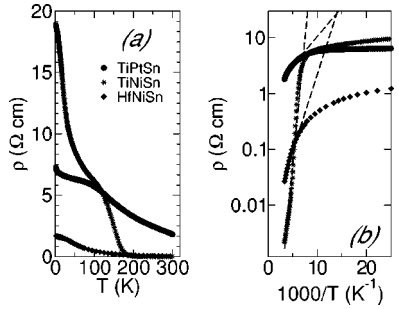

FIG. 3. (a) Temperature dependent resistivities of single crystal TiPtSn (filled circles), TiNiSn (stars), and HfNiSn (filled diamonds). (b) Activation plots for the same data. Dashed lines are activation fits over the indicated temperature ranges.

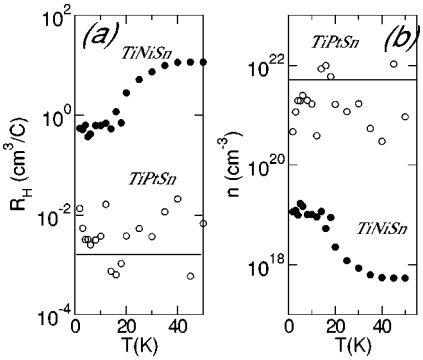

FIG. 4. (a) Hall constants R_H and (b) the corresponding single band electron concentrations n for TiNiSn and TiPtSn single crystals. Solid lines indicate upper limit for R_H and lower limit for n for single crystal HfNiSn.

a constant value at the lowest temperatures, but in addition there are regions of distinctly different slopes, especially for TiNiSn. These results indicate the presence of narrow bands of impurity/defect states in the semiconducting gap, with excitation energies which are smaller than the semiconducting gap itself. The highest temperature transport gaps are very small: 26 meV for HfNiSn, 28 meV for TiPtSn, and 79 meV for TiNiSn. The estimates for the transport gaps in HfNiSn and TiNiSn single crystals are much smaller than the values previously reported for polycrystals[1] and single crystal TiNiSn (Ref. 16) carried out to temperatures as large as 1000 K. In addition, they are smaller than the indirect gap of 0.5 eV predicted by electronic structure calculations for TiNiSn and HfNiSn.[13] These observations support our expectation that the transport gap represents activation from impurity or defect states to the conduction band edge, differing considerably from sample to sample.

Hall effect measurements have been carried out on single crystals of HfNiSn, TiNiSn, and TiPtSn, in order to estimate the number and type of carriers present. The data are presented in Fig. 4(a). No Hall signal was detected in single crystal or polycrystalline HfNiSn in fields as large as 9 T, and for temperatures between 1.2 and 12 K. Our experimental accuracy consequently yields only an lower bound for a single band carrier concentration n of 5×10^{21} cm^{-3}, which is more than one carrier per unit cell. The Hall constant in TiPtSn is just at the limits of our experimental resolution, and also indicates a large carrier concentration $\sim1\times10^{21}$ cm^3. In view of the semiconducting characters revealed in the resistivity of single crystal HfNiSn and TiPtSn, we view these single band carrier concentrations as unreasonably high. We consider it more likely that both HfNiSn and TiPtSn are very close to perfect compensation, and perhaps may even be semimetals. In contrast, a large Hall voltage was detected in TiNiSn, linear in field and with a slope which indicates that the dominant carriers are electrons, although at high temperatures R_H is about twice the value previously reported.[16] The temperature dependence of the electron concentration n deduced from these measurements is plotted in Fig. 4(b), showing a strong increase with reduced temperature, amounting to an increase by approximately one electron per 365 unit cells between 40 K and the approxi-

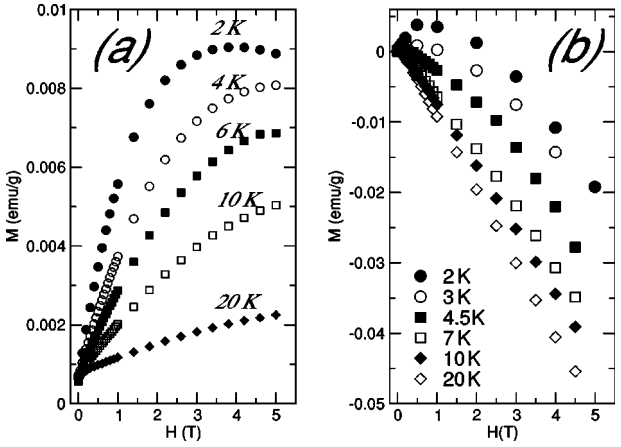

FIG. 5. (a) Magnetization $M(H)$ of a HfNiSn polycrystal annealed at 1000 °C for 720 h, and a TiNiSn single crystal (b). Note the large diamagnetic magnetization in (b), and the relatively much smaller diamagnetic contribution in (a), evident only in the 2 K $M(H)$ curve above 3 T.

mately constant value of 1×10^{19} cm^{-3} found below 15 K. It is significant that the low-temperature electron concentration in TiNiSn is approximately the same as the number of paramagnetic moments inferred from the magnetization measurements, which we discuss next.

All of the single crystal and polycrystalline samples we measured are weakly magnetic, despite the nominally nonmagnetic character expected for the filled-*d* shell half-Heusler compounds. The field dependence of the magnetization of polycrystalline HfNiSn, annealed for 720 h at 1000 °C, is presented in Fig. 5(a), while similar data for single crystal TiNiSn appear in Fig. 5(b). In both cases, the magnetization is strongly nonlinear, especially at low fields and low temperatures. As the temperature is raised, the magnetization is increasingly dominated by a diamagnetic contribution, linear in field, which is especially evident for the TiNiSn sample. The magnetization M divided by a constant measuring field of 1.5 T is plotted in Fig. 6 as a function of temperature for three different samples: polycrystalline HfNiSn, both as cast and annealed for 720 h at 1000 °C, as

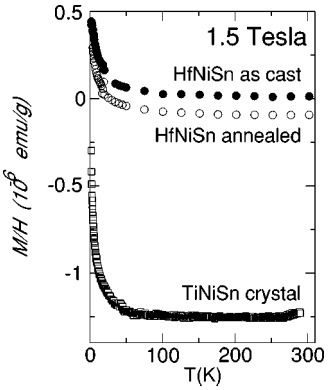

FIG. 6. Temperature dependence of the magnetization M divided by a 1.5 T measuring field H for polycrystalline HfNiSn, both as cast and annealed for 720 h at 1000 °C, and for a single crystal of TiNiSn.

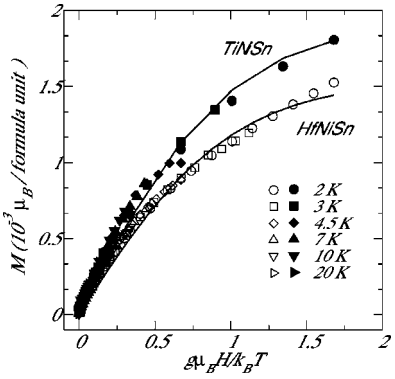

FIG. 7. Magnetization sweeps, corrected for a linear diamagnetic susceptibility, collapse onto scaling curves as a function of $g\mu_B H/k_B T$, for both polycrystalline HfNiSn (annealed at 1000 °C for 720 h) and single crystal TiNiSn. The solid lines are $J=1/2$ Brillouin functions.

well as single crystal TiNiSn. Figure 6 shows that the paramagnetic contribution to the magnetization is largest at low temperatures, but is superposed on a diamagnetic contribution. It is evident that the magnitudes of the paramagnetic and diamagnetic components, as well as their relative weights, vary considerably among the samples we investigated.

Figures 5 and 6 suggest that it may be possible to separate the two components of the magnetization by modelling the magnetization in each sample as $M(H,T)=\chi_0 H+\mathcal{F}(H/T)$. The first term represents a field independent susceptibility, which we will show combines the normal diamagnetic susceptibility of the semiconducting host, with an additional Pauli paramagnetic susceptibility, which varies among samples. Given the small magnitude of the moments shown in Fig. 5, we think it unlikely that long range magnetic order is responsible for the nonlinear magnetization found at low temperatures. Instead, we suggest that the second term represents the scaling behavior of isolated and localized magnetic moments, where $\mathcal{F}$ is consequently expected to be the Brillouin function.

The results of this modeling are shown in Fig. 7, which demonstrates that the magnetization sweeps taken in both samples for temperatures which range from 2–20 K collapse onto scaling curves if a diamagnetic term is previously subtracted from the data at each temperature. As indicated, the scaled and corrected magnetizations for HfNiSN and TiNiSn are well described by $J=1/2$ Brillouin functions, yielding moment densities of $1.98\times10^{-3}\mu_B$ per formula unit TiNiSn and $1.55\times10^{-3}\mu_B$ and $0.144\mu_B$ per formula unit HfNiSn for the two annealed and polycrystalline HfNiSn samples investigated. We find that the diamagnetic susceptibilities χ_0 of the three systems are also very different, as Fig. 6 suggests. These susceptibilities are plotted in Fig. 8, showing that $|\chi_0|$ is much larger for TiNiSn than for either HfNiSn sample, although $|\chi_0|$ varies by almost an order of magnitude between the two HfNiSn samples. While χ_0 approaches a constant value at low temperature in one of the polycrystalline HfNiSn samples (filled circles), in each of the three samples, $|\chi_0|$ increases approximately linearly with temperature.

The pronounced temperature and sample dependences of

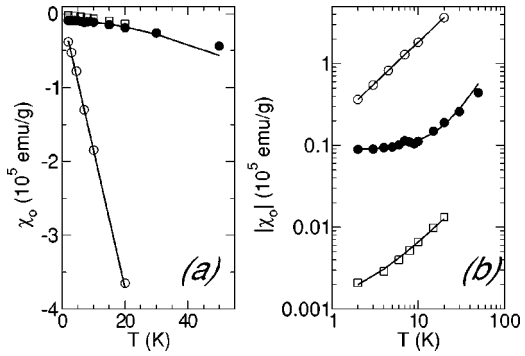

FIG. 8. (a) The temperature dependence of the diamagnetic susceptibility χ_0 for annealed samples of polycrystalline HfNiSn (filled circles and open squares) and single crystal TiNiSn (open circles) Solid lines are power law fits, demonstrated in a double logarithmic plot in (b). The slopes of the power law fits to $|\chi_0|$ are 1.0 for one HfNiSn (filled circles) and TiNiSn, and 1.8 for the other HfNiSn polycrystalline sample (open squares).

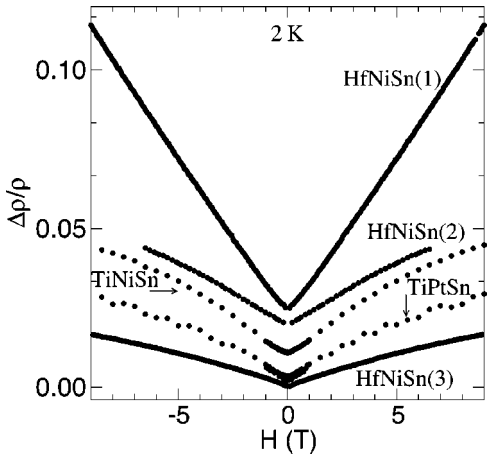

FIG. 9. The magnetoresistances of single crystals of HfNiSn [HfNiSn(3)], TiPtSn, and TiNiSn at 2 K. For comparison, data are shown for polycrystalline samples of HfNiSn, both as-cast [HfNiSn(1)] and annealed for 720 h at 1000 °C [HfNiSn(2)]. The TiNiSn, TiPtSn, and polycrystalline HfNiSn data have all been offset for comparison.

χ_0 which are demonstrated in Fig. 8 argue strongly for the presence of a paramagnetic contribution to the magnetization which is linear in field. The susceptibility of a semiconductor is approximated by the sum of the core susceptibilities of the constituent atoms: -4.8×10^{-5} emu/g for HfNiSn and -3.7×10^{-5} for TiNiSn,[17] and is consequently independent of temperature and invariant among samples of the same nominal composition. The values we find for χ_0 in HfNiSn and TiNiSn do not approach these limits on the temperature range of our experiment, suggesting the presence of an additional positive magnetization, linear in field and decreasing in magnitude with increasing temperature. The variation of χ_0 between the two HfNiSn samples suggests that this inferred positive susceptibility has an extrinsic origin, consistent with the small magnitude of the local moments found in each sample, and with the variations in moment concentrations found among different samples.

We conclude that there are two magnetic entities present with different relative weights in each of our half-Heusler samples, superposed on the diamagnetic response of the semiconducting host. The first entities are localized magnetic moments, perhaps generated by the inevitable site disorder characteristic of the half-Heusler structure. Still, the level of this putative disorder can be quite low, corresponding to only one defect per 7000 unit cells in our least magnetic HfNiSn sample. Secondly, we propose that there are also extended and metallic states present which are responsible for the inferred paramagnetic susceptibility. In agreement with Hall effect measurements on TiNiSn, the number of these metallic states grows with decreasing temperature. It is interesting that the electron concentration in TiNiSn is similar to the concentration of localized magnetic moments, suggestive that both have the same origin, presumably defects or impurities. Further, the data suggest that the electron contributed by each impurity or defect in TiNiSn ultimately becomes delocalized as $T\rightarrow0$. We speculate that this loss of magnetism at low temperatures may result from Kondo compensation of the moment bearing impurities by the itinerant carriers which originate with impurities or defects.

Perhaps the most striking property of the nonmetallic half-Heusler compounds is their magnetoresistance, which is linear or even sublinear in field at the lowest temperatures. The anomalous magnetoresistance has been observed in every half-Heusler compound we have measured, both single crystals and polycrystals, both as cast and annealed. This is demonstrated in Fig. 9 which presents the 2 K magnetoresistances of HfNiSn, TiPtSn, and TiNiSn single crystals, and HfNiSn polycrystal, both as cast and annealed for 720 h at 1000 °C. The magnetoresistances of the single crystal samples are markedly sublinear, while those of the polycrystalline samples are more highly linear. In neither case is there any suggestion of a quadratic magnetoresistance, down to fields as small as 1000 Oe. We note that trace superconductivity in the polycrystalline samples prohibits measurements to fields less than ~500 Oe. The magnitude of the magnetoresistance is rather modest, amounting to a few percent in each of the crystalline samples. It approaches 10% at 9 T in the as-cast polycrystalline sample, although annealing reduces the magnetoresistance to the level observed in the single crystals. This may result either from a compactification of the internal structure of the polycrystals, since annealing removes conducting grain boundaries, or from rendering the HfNiSn grains more nearly stoichiometric, as in the single crystal.

The low field magnetoresistance of all samples ultimately becomes quadratic in field if the temperature is increased sufficiently. The longitudinal magnetoresistance of single crystal HfNiSn is presented at several temperatures in Fig. 10, with an expanded low field region in the inset. At 2 K, the magnetoresistance is sublinear over our entire field range, and is never quadratic, even at the lowest fields. At 4 K, the magnetoresistance is linear over virtually the entire range of fields studied, with little trace of the upward curvature which emerges at the lowest fields at 6 K. Raising the temperature still furthur yields a range of fields for which quadratic magnetoresistance is found. This is demonstrated in Fig. 11, where the magnetoresistance of single crystal HfNiSn is

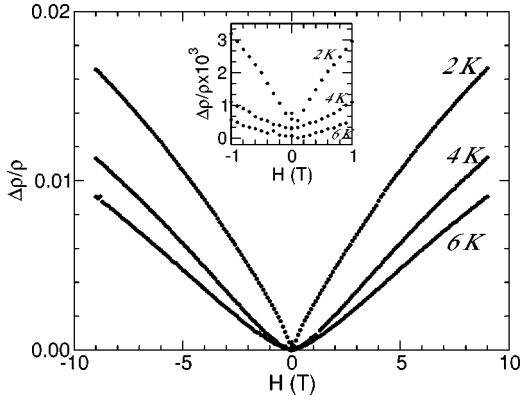

FIG. 10. The magnetoresistance $\Delta\rho/\rho$ for single crystal HfNiSn at different fixed temperatures. The inset shows the same data for an expanded range of low fields. The 2 and 4 K data in the inset have been offset vertically for comparison.

plotted as a function of H^2. At 30 K and above, the magnetoresistance is quadratic in field for the entire range of fields studied, 0.01–9 T. As the temperature is lowered, clear departures from $\Delta\rho/\rho \propto H^2$ are observed, below fields H^* which become progressively smaller as the temperature is reduced. This analysis has been repeated on all of our samples, and the results are summarized in Fig. 12. It is evident that the range of fields $H \leqslant H^*$ and temperatures for which $\Delta\rho/\rho \propto H^2$ varies considerably among the different samples. For instance, the magnetoresistance of the annealed sample of HfNiSn (open circles, Fig. 12) is quadratic in fields up to 9 T for all temperatures above 15 K, while clear departures are still evident at temperatures as large as 100 K for an as cast polycrystalline sample of HfNiSn (open squares, Fig. 12).

Figure 12 may be viewed as an organizational scheme for our magnetoresistance observations, analagous to a phase diagram, where $H^*(T)$ represents a crossover from a regime at low fields where the magnetoresistance is quadratic in field, to a regime at high fields where the magnetoresistance is linear or even sublinear in field. In agreement with the

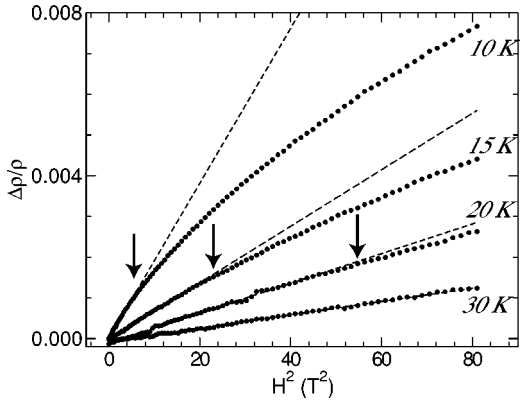

FIG. 11. The magnetoresistance of a single crystal of HfNiSn plotted as a function of the field squared at different temperatures. Vertical arrows indicate the highest field H^* at which quadratic field dependences are observed, and the dashed lines are linear fits to the data having $H \leqslant H^*$.

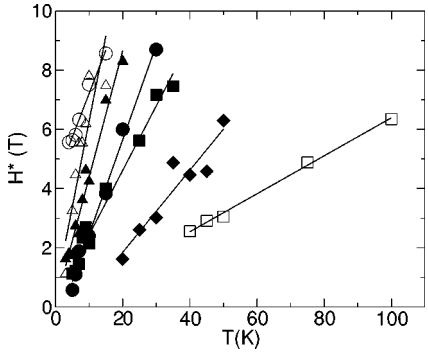

FIG. 12. $H^*(T)$ defines a crossover from quadratic magnetoresistances at low fields to linear or sublinear magnetoresistance at high fields. H^* varies substantially among the different samples: Single crystal HfNiSn (filled circles), two different annealed polycrystalline HfNiSn samples (open circles, filled squares), and the corresponding two different as cast polycrystalline HfNiSn (filled diamonds, open squares), and single crystals of TiNiSn (filled triangles) and TiPtSn (open triangles).

discussion of Fig. 9, the linear magnetoresistance is seen for the widest range of temperatures in the as cast polycrystalline samples, while annealing confines the linear magnetoresistance to the lowest temperatures and highest fields. $H^*(T)$ for the single crystals is similar to that of the most homogeneous polycrystalline samples, which have been annealed for the longest times.

The observation of a linear or sublinear magnetoresistance is anomalous, as the magnetoresistance typically depends on the field magnitude, yielding a magnetoresistance which is even and usually quadratic in the applied field. Nonetheless, there are a few circumstances in which a linear magnetoresistance is expected. A linear magnetoresistance can occur in inhomogeneous materials, resulting from the accidental admixture of the Hall signal.[18] We rule out this possibility for the half-Heuslers, as we observe linear magnetoresistance in single crystals, and further since the Hall signal is immeasurably small, especially in HfNiSn and TiPtSn. Similarly, a variety of different mechanisms can lead to linear magnetoresistance in systems with large carrier concentrations,[19,20] but in most cases their application to the minimally magnetic and essentially semiconducting half-Heuslers seems tenuous. Finally, we note that there is no evidence for either magnetic or structural transitions, which might provide an internal symmetry breaking field, superseding the applied field.

Linear magnetoresistance is expected in metals with closed Fermi surface orbits at intermediate fields, in a crossover regime between the quadratic magnetoresistance expected at low fields, and saturation at high fields. The range of fields over which linear magnetoresistance can be observed is potentially quite extensive for materials with a high degree of compensation.[21] However, this linear crossover regime emerges when the product of the cyclotron frequency ω_c and the scattering time τ exceeds one $\omega_c\tau \geqslant 1$. For TiNiSn at 2 T, where $n=1.3\times10^{19}$ and $\rho=18\Omega$-cm, $\omega_c\tau=1$ for an applied field of 3.7×10^5 T. Indeed, this crossover field could be considerably larger if we consider that the Hall measurements provide only a lower bound on the total num-

ber of carriers, which may be electrons as well as holes. Conversely, if we assume that this crossover field is no more than 100 Oe, consistent with our lowest temperature magnetoresistance results on single crystal HfNiSn and TiPtSn, we would require a total carrier concentration of $\sim 3 \times 10^{13}$ cm^{-3}. It is difficult to believe that the numbers of electrons and holes present in both our single crystal and polycrystalline samples are balanced at the level of one carrier per 10^8 unit cells, as the absence of a Hall signal suggests. We are forced to conclude that in each of our samples, linear or sublinear magnetoresistance is observed for a wide range of fields which are comfortably in the low field limit $\omega_c \tau \ll 1$.

Linear magnetoresistance is also predicted theoretically for a low density electron gas, in which only the lowest Landau level is occupied.[22–24] The two requirements for realizing this quantum magnetoresistance are that $H \geqslant (\hbar cn)^{2/3}$ and that $T \ll eH\hbar/m^*c$. Consequently, the linear magnetoresistance should only be observed in TiNiSn at fields greater than 36 T, and for temperatures $T \ll 1.35\ (K/T)H$. It is possible that the latter condition is satisfied in the half-Heusler compounds, since as Fig. 11 demonstrates, the linear magnetoresistance is only observed above a field H^* which increases linearly with temperature. In this view, the different slopes found in the plot of $H^*(T)$ for the different systems (Fig. 11) could plausibly be the result of variations in magnitude of the effective mass between the least massive ($m/m = 0.09$ in as cast HfNiSn 99106) and the heaviest ($m/m = 0.58$ in single crystal TiPtSn). Nonetheless, our observation of linear magnetoresistance in TiNiSn in fields as small as 0.01 T, where the criterion $H \geqslant (\hbar cn)^{2/3}$ is dramatically violated is problematic for the quantum magnetoresistance theory as well. The central dilemma lies with explaining the unexpected persistance of the linear and sublinear magnetoresistance to extremely low fields, particularly at low temperatures. If the linear magnetoresistance observed in the half-Heuslers derives from the scattering of fully quantum mechanical states, then our measurements suggest a less restrictive set of necessary conditions than has been theoretically proposed.

Alternative views have suggested that compositional inhomogeneities may be required to explain the linear magnetoresistance.[23,29] One possibility is that only a tiny fraction of the carriers detected by the Hall effect in TiNiSn, one carrier in $\sim 2 \times 10^5$, actually participates in the quantum magnetoresistance. We note that a similar explanation has been proposed[23] as an explanation for the linear magnetoresistance observed in doped silver chalcogenide compounds.[25–28] Here, spatial separation of conducting and insulating regions was invoked to achieve the needed reduction in effective carrier concentration, a scenario which is likely inapplicable to the single crystal half-Heuslers. A more recent theoretical proposal[29] relates the magnitude of the linear magnetoresistance to the average spatial variance in the carrier mobility $\Delta\mu$ from its mean value $\langle\mu\rangle$. We think this theory captures a number of features of the linear magnetoreststance found in the half-Heuslers. In this scenario, the as-cast HfNiSn polycrystalline samples have the least uniform mobility and composition, and annealing improves the overall homogeneity, reducing $\Delta\mu$ and also the linear magnetoresistance, which is much smaller in the single crystal samples. Similarly, increasing temperature reduces the overall mobility and perhaps its variance as well, leading to the suppression of the linear magnetoresistance in all samples evident in Figs. 10 and 11.

It is still unclear whether the linear magnetoresistances found in the half-Heuslers and the silver chalcogenides arise from the same fundamental mechanism. Certainly there are general resemblences between the doped silver chalcogenides and the semiconducting half-Heuslers, as both systems are nonmagnetic semiconductors, with small or vanishing values of the Hall constant. We note that the single crystal half-Heuslers generally have larger resistivities, and as far as is known, electron concentrations which are similar to those in optimally doped $Ag_{2-\delta}Te$.[26] The progression of the magnetoresistance from sublinear, to linear, and ultimately to quadratic field dependencies is achieved by increasing temperature and consequently decreasing electron concentration in the half-Heuslers. In contrast, temperature has a very modest effect on the linear magnetoresistance found in the doped silver chalcogenides,[27] although the same progression of field dependencies is achieved in this system by using high pressures to drive the Hall constant through zero.[26] A similar sensitivity to carrier density is apparently absent in the half-Heuslers, since the magnetoresistances of single crystal HfNiSn, TiPtSn, and TiNiSn are very similar in magnitude, despite their very different electron concentrations. Finally, we note that the linear magnetoresistances of the single crystal and polycrystal half-Heuslers are much smaller than those of the silver chalcogenides, consistent with a much higher degree of electronic homogeneity.[23,26,29]

We have established here that single crystals of several half-Heusler compounds, selected to have a total of 18 valence electrons, are small gap insulators, in agreement with both electronic structure calculations. Resistivity measurements show that HfNiSn, TiPtSn, and TiNiSn single crystals are all semiconducting, while magnetization measurements argue that both localized magnetic and extended states are introduced with impurities or site interchange disorder. Hall effect measurements indicate that the number of electrons and holes is closely balanced in HfNiSn and TiPtSn, although there is a pronounced excess of electrons in TiNiSn. Both the corresponding electron concentration and the inferred Pauli susceptibility in TiNiSn increase with decreasing temperature, which may signal the return via the Kondo effect of electrons to the Fermi surface which were formerly localized at high temperatures in magnetic impurity states.

Our results deepen the mystery surrounding the origin of linear magnetoresistance in materials with small carrier densities. Neither the classical nor quantum mechanical theories of the magnetoresistance can countenance the persistance of the linear magnetoresistance to fields as low as 0.01 T, given the mobility and carrier densities characteristic of both half-Heuslers and the doped silver chalcogenides. The suppression of the linear magnetoresistance in the half-Heuslers with annealing in polycrystalline samples, and in single crystals, as well as with increased temperature are in qualitative agreement with a theoretical proposal[29] that spatial variations in the mobility and its variance are responsible for the linear magnetoresistance.

We acknowledge stimulating discussions with C. M. Varma, as well as the assistance of S. Ramakrishnan in early stages of the sample synthesis. M.C.A. is grateful to the Dutch NWO and FOM for partial support during a sabbatical visit to Leiden University, where this project was initiated. Work at the University of Michigan was performed under the auspices of the U.S. Department of Energy under Grant No. DE-FG02-94ER45526. M.C.B. acknowledges partial financial support from NHMFL-Los Alamos. E.M.S. acknowledges partial financial support from CONACYT (Mexico) through Grant No. 39643-F. This manuscript has been authored by Iowa State University of Science and Technology under Contract No. W-7405-ENG-82 with the U.S. Department of Energy.

[1] F. G. Aliev, N. B. Brandt, V. V. Moshchalkov, V. V. Kozyrkov, R. V. Skolozdra, and A. I. Belogorokhov, Z. Phys. B: Condens. Matter **75**, 167 (1989).
[2] F. G. Aliev, V. V. l Kozyrkov, V. V. Moschalkov, R. V. Skolozdra, and K. Durczewski, Z. Phys. B: Condens. Matter **80**, 353 (1990).
[3] B. A. Cook, J. L. Harringa, Z. S. Tan, and W. A. Jesser (unpublished).
[4] C. Uher, J. Yang, S. Hu, D. T. Morelli, and G. P. Meisner, Phys. Rev. B **59**, 8615 (1999).
[5] H. Hohl, A. P. Ramirez, C. Goldmann, G. Ernst, B. Wolfling, and E. Bucher, J. Phys.: Condens. Matter **110**, 7843 (1998).
[6] K. Mastronardi, D. Young, C.-C. Wang, P. Khalifah, R. J. Cava, and A. P. Ramirez, Appl. Phys. Lett. **74**, 1415 (1999).
[7] J. Tobola, J. Pierre, S. Kaprzyk, R. V. Skolozdra, and M. A. Kouacou, J. Phys.: Condens. Matter **10**, 1013 (1998).
[8] M. Kasaya, H. Suzuki, T. Yamaguchi, and K. Katoh, J. Phys. Soc. Jpn. **61**, 4187 (1992).
[9] A. E. Dwight, J. Less-Common Met. **39**, 341 (1974).
[10] H. Hohl, A. P. Ramirez, C. Goldmann, G. Ernst, B. Wolfling, and E. Bucher, J. Phys.: Condens. Matter **11**, 1697 (1999).
[11] J. Pierre, R. V. Skolozdra, Yu. K. Gorelenko, and M. Kouacou, J. Magn. Magn. Mater. **134**, 95 (1994).
[12] J. Tobola, J. Pierre, S. Kaprzyk, R. V. Skolozdra, and M. A. Kouacou, J. Magn. Magn. Mater. **159**, 192 (1996).
[13] S. Ogut and K. M. Rabe, Phys. Rev. B **51**, 10 443 (1995).
[14] A. Slebarski, A. Jezierski, A. Zygmunt, S. Mahl, and M. Neumann, Phys. Rev. B **57**, 9544 (1998).
[15] P. C. Canfield and Z. Fisk, Philos. Mag. B **65**, 1117 (1992).
[16] F. G. Aliev, Physica B **171**, 199 (1991).
[17] P. W. Selwood, *Magnetochemistry*, 2nd ed. (Interscience Publishers, New York, 1956), p. 78.
[18] C. Herring, J. Appl. Phys. **31**, 1939 (1960).
[19] For a review of mechanisms which can lead to linear magnetoresistance in metals,see S. L. Bud'ko, P. C. Canfield, C. H. Mielke, and A. H. Lacerda, Phys. Rev. B **57**, 13 624 (1998).
[20] D. P. Young, R. G. Goodrich, J. F. DiTusa, S. Guo, P. W. Adams, J. Y. Chan, and D. Hall, cond-mat/0305116v1 (unpublished).
[21] A. B. Pippard, *Magnetoresistance in Metals* (Cambridge University Press, New York, 1989), p. 29.
[22] A. A. Abrikosov, Sov. Phys. JETP **36**, 127 (1969).
[23] A. A. Abrikosov, Phys. Rev. B **58**, 2788 (1998).
[24] A. A. Abrikosov, Europhys. Lett. **49**, 789 (2000).
[25] A. Husmann, J. B. Betts, G. S. Boebinger, A. Migliori, T. F. Rosenbaum, and M.-L Saboungi, Nature (London) **417**, 421 (2002).
[26] M. Lee, T. F. Rosenbaum, M.-L Saboungi, and H. S. Schnyders, Phys. Rev. Lett. **88**, 066602 (2002).
[27] R. Xu, A. Husmann, T. F. Rosenbaum, M.-L Saboungi, J. E. Enderby, and P. B. Littlewood, Nature (London) **390**, 57 (1997).
[28] H. S. Schnyders, M.-L Saboungi, and T. F. Rosenbaum, Appl. Phys. Lett. **76**, 1710 (2000).
[29] M. M. Parish and P. B. Littlewood, Nature (London) **426**, 162 (2003).